

FULL TEMPERATURE MAPPING SYSTEM FOR STANDARD 1.3 GHZ 9-CELL ELLIPTICAL SRF CAVITIES*

T. Tajima[#], A. Bhatt, A. Canabal, P. Chacon, G. Ereemeev, R. Roybal, J. Sedillo
LANL, Los Alamos, NM 87545, U.S.A.

Abstract

A full temperature mapping system with 4608 100-ohm Allen-Bradley resistors has been built and tested at LANL. With this temperature mapping system we were able to locate lossy regions in the 1.3 GHz 9-cell SRF cavity due to field emission and direct heating. The results of the temperature mapping, their correlation with the inside surface anomalies will be shown together with Q_0 - E_{acc} curves.

INTRODUCTION

The *in-situ* temperature mapping (T-map) of SRF cavity outside surface during cryogenic testing has been one of the best cavity diagnostic tools. For multi-cell cavities and large cavities, due to the large number of sensors required to cover enough areas, a rotating-arm type systems have been used at, e.g., DESY [1] and KEK [2]. Recently, however, at some institutions such as LANL, FNAL and JLab, a fixed-type system has been extended to multi-cell cavities [3-5]. The major advantage for a fixed-type system is its speed of data acquisition. At LANL, we have successfully developed and commissioned our system for standard-shape 1.3 GHz 9-cell cavities.

T-MAP SYSTEM

The details of the system are described in Refs. [3] and [4]. In order to reduce the heat leak and the size of signal cables, 768 28-AWG manganin wires were used through a custom-made KF40 connector sealed with Stycast 2850FT. A total of 4608 100Ω Allen Bradley carbon resistors surround the cavity. Due to the present data taking capacity, the cavity surface was electronically divided into 9 sectors in the azimuthal direction. Figure 1 shows the cavity with all T-map boards attached.

CAVITY TEST RESULTS

A 9-cell cavity AES003 was loaned from FNAL for the commissioning of our T-map system. The detailed description of the result can be found in Ref. [6]. Here, we show some highlights.

Figure 2 shows the Q_0 - E_{acc} curve of the cavity. The cavity was limited by field emission (FE). The one data at ~ 8.7 MV/m was obtained after some RF processing.

T-map Results

We observed a line-like heating along one meridian in cell 2 at 30° , which seems to have occurred due to FE. By changing the cavity mode, we were able to see other

heating spots. Figure 3 shows the field levels in each cell at different modes.



Figure 1: A 1.3 GHz, 9-cell cavity with T-mapping boards supporting plates (left) and full assembly of boards around the cavity (right).

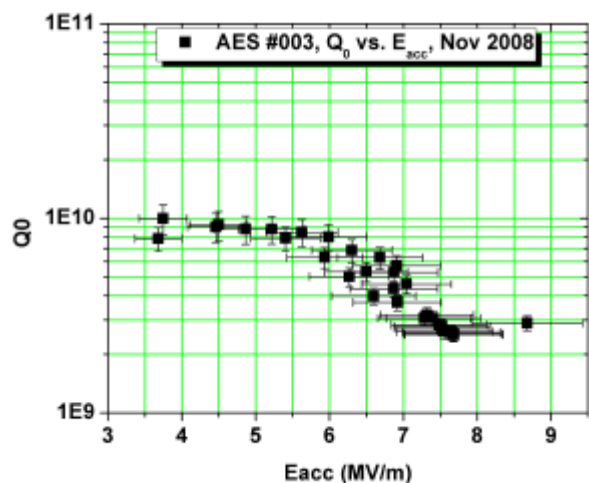


Figure 2: Q_0 - E_{acc} curve of a 9-cell cavity.

Figure 4 shows a collection of heating spots at different modes. As one can expect from Fig. 3, some heating spots were observed at $6/9\pi$ mode since there is no electric field in cell 2. One interesting observation was that we saw a heating spot in cell 8 where there is no electromagnetic field. It is suspected that the electrons

*Work supported by DTRA

[#]tajima@lanl.gov

due to FE in cell 9 flew into cell 8 and bombarded the surface causing this heating.

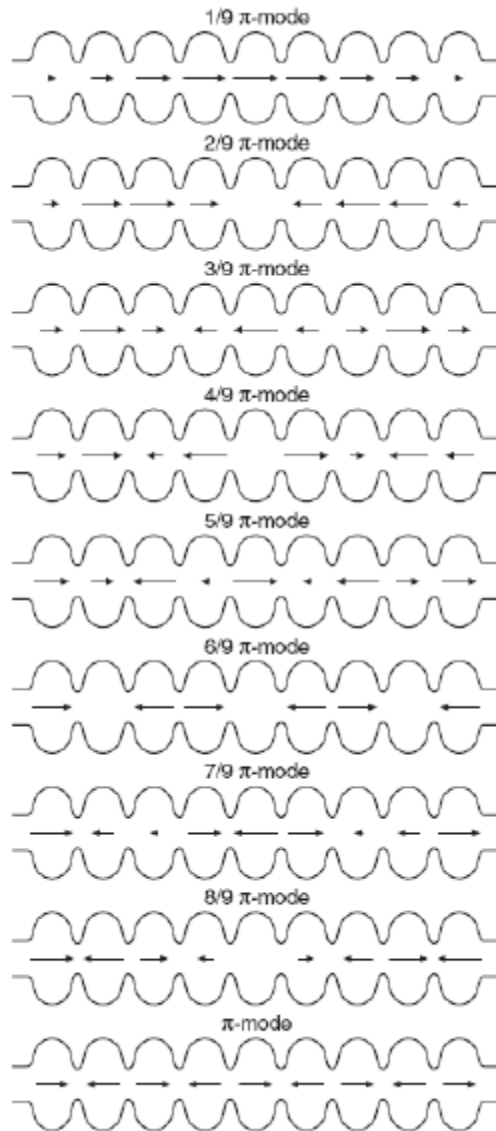


Figure 3: Cavity modes. The direction and length of an arrow represent the direction of electric field and strength at an instant, respectively [7].

Correlation with Surface Inspection Results

After cryogenic testing, the cavity was moved into our clean room with the vacuum valve closed. The cavity was then vented with filtered nitrogen. After all the flanges were removed, the cavity was set on our surface inspection system [8] and inspected. Figure 5 illustrates our inspection system. It consists of a Karl Storz 6 mm diameter video scope tip (working distance 7-40 mm) with remote articulation.

We found defects at most of the heating spots. Figure 6 shows a defect on the stiffening ring welding line that seems to be responsible for the FE in π mode.

Figure 7 shows the defects that seem to be responsible for the heating in cell 2 in $7/9\pi$ mode.

Figures 8 and 9 show the defects that seem to be responsible for the heating spots in cells 7 and 9, respectively.

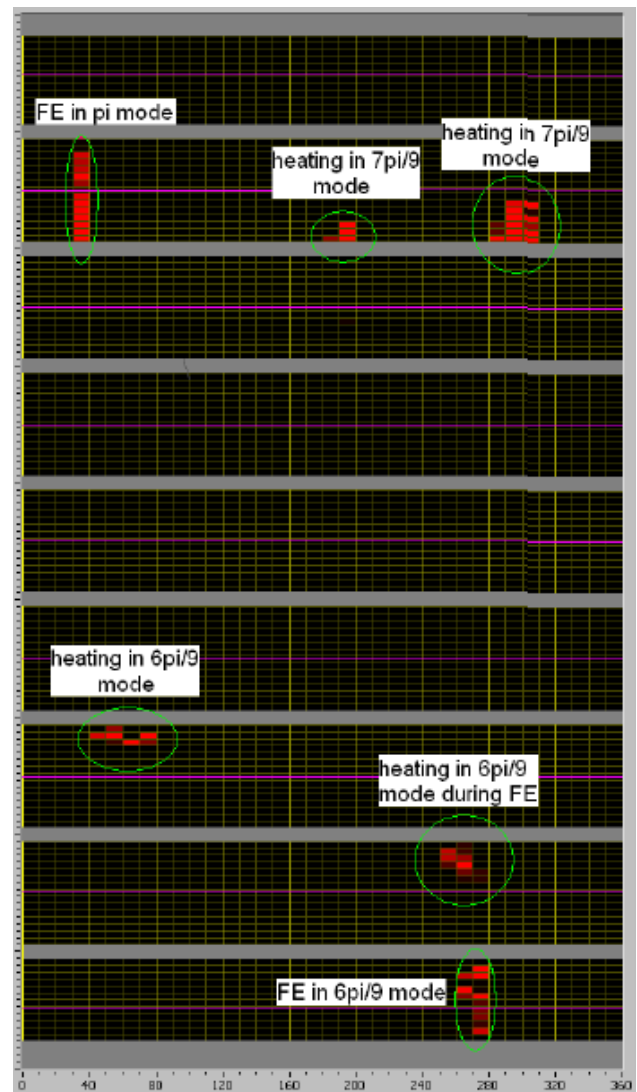


Figure 4: A summary of 2D temperature maps taken at different cavity modes. The magenta line shows the equator of each cell. FE denotes field emission.

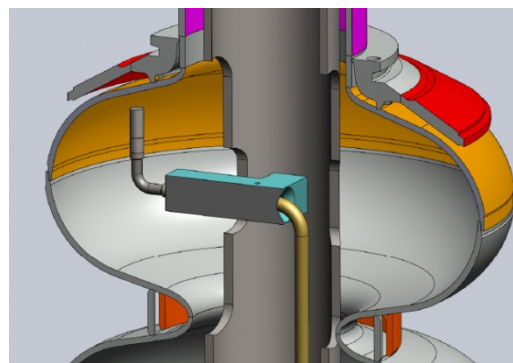


Figure 5: Cavity inner surface inspection using a video scope [8].

No defect was found at the heating spot in cell 8 in $6/9\pi$ mode. This supports the hypothesis of heating by the electrons emitted from the FE source in cell 9.



Figure 6: A defect found on a stiffening ring welding area in cell 2 at 30° that seems responsible for FE in π mode.

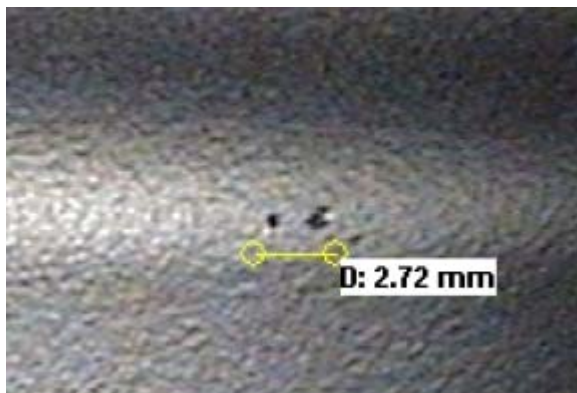


Figure 7: Defects found on the bottom surface of cell 2 at 190° that seem to be responsible for the heating in $7/9\pi$ mode.



Figure 8: Two scratches found on the iris between cells 6 and 7 at 70° that seem to be responsible for the heating in $6/9\pi$ mode.

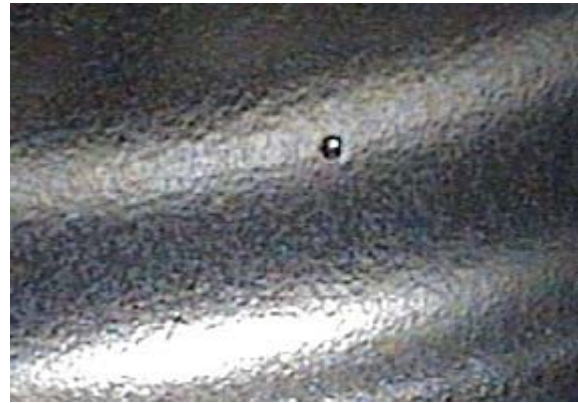


Figure 9: A defect found on the bottom of cell 9 at 260° that seems to be responsible for the heating due to FE in $6/9\pi$ mode.

FUTURE PLAN

We plan to develop a similar T-map system using silicon diodes as sensors to replace the obsolete Allen Bradley resistors. Also, if funded, we would like to develop a system to locally repair the defects to improve the cavity performance.

REFERENCES

- [1] Q.S. Shu et al., "An Advanced Rotating T-R mapping & its Diagnoses of TESLA 9-cell Superconducting Cavity," PAC'95, Dallas, TX, May 1995, p. 1639 (1996); <http://www.JACoW.org>.
- [2] H. Sakai et al., "Cavity Diagnostics Using Rotating Mapping System for L-Band ERL Superconducting Cavity," *ibid.* [2], p. 907.
- [3] A. Canabal et al., "Development of a Temperature Mapping System for 1.3-GHz 9-Cell SRF Cavities," PAC'07, Albuquerque, June 2007, p. 2406 (2007); <http://www.JACoW.org>.
- [4] A. Canabal et al., "Full Real-Time Temperature Mapping System for 1.3 GHz 9-cell Cavities," EPAC'08, Genoa, June 2008, p. 841 (2008); <http://www.JACoW.org>.
- [5] P. Kneisel, "Update on R&D Activities in the Americas," TTC meeting, Delhi, India, 20-23 October 2008; <https://indico.desy.de/materialDisplay.py?contribId=8&sessionId=1&materialId=slides&confId=946>.
- [6] G. Ereemeev et al., "Report on AES 003 1.3 GHz 9-cell Superconducting Niobium Cavity Test Results at LANL," LANL Report LA-UR-09-01090; http://laag.lanl.gov/scrflab/pubs/ILC/LA-UR-09-01090_AES_003_test_final_report_rev_1_1.pdf.
- [7] E. Vogel, "High gain proportional rf control stability at TESLA cavities," *Phys. Rev. ST AB* 10 (2007) 052001.
- [8] T. Tajima et al., "Conceptual Design of Automated Systems for SRF Cavity Optical Inspection and Assembly," *ibid.* [2], p. 922.